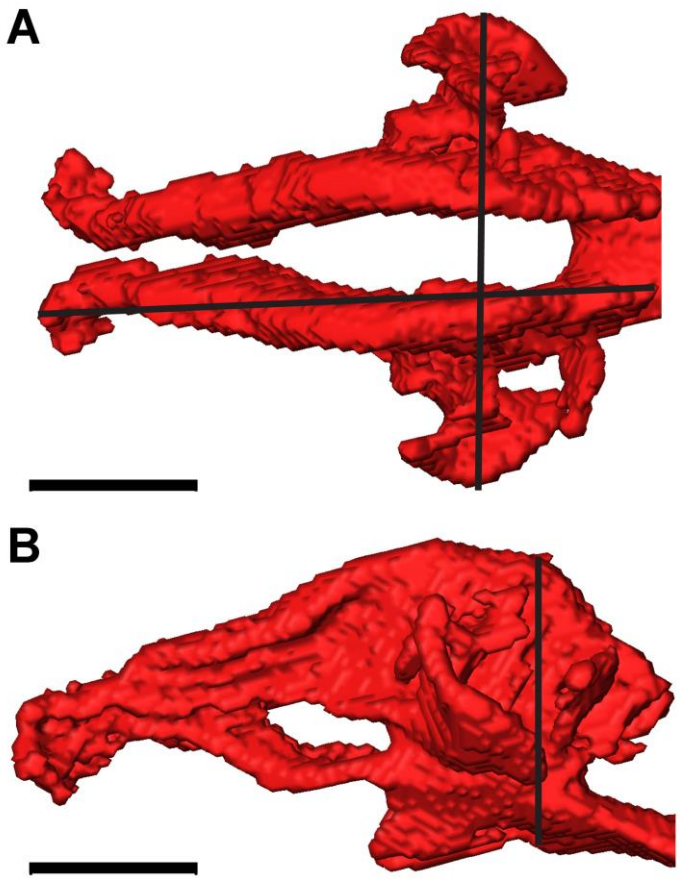

Fig. S1. Linear measurements within nasal passage endocasts. (A) Dorsal and (B) lateral view of 3D reconstructions of MRM images of an endocast of the segmented nasal passages from an unaffected, P0 *Fgfr2*$^{+/+}$ mouse. Black lines indicate positions for measurements of nasal passage (A) length and width, and (B) height presented in Table S2. Anterior is to the left. Scale bars: 1 mm.

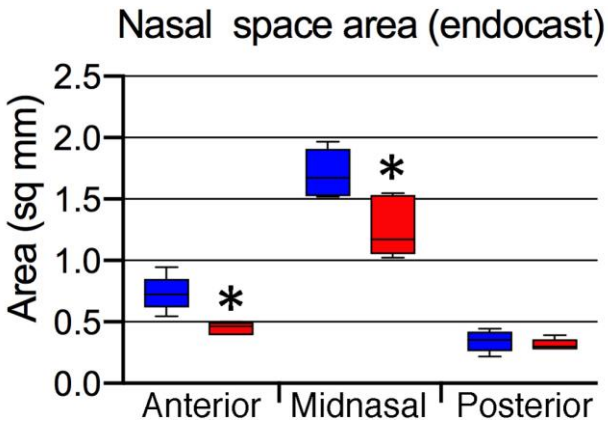

Fig. S2. Decreases in cross-sectional area of nasal airspace endocasts in the Apert *Fgfr2*$^{+/S252W}$ line. The cross-sectional area of the nasal passages at anterior, midnasal and posterior locations was determined from MRM endocast slices. Blue boxes, unaffected littermates; red boxes, mutant. *n*=5. Data are presented as the median, 25th and 75th percentiles; whiskers indicate minimum and maximum values. **P*<0.05 (Student's *t*-test).

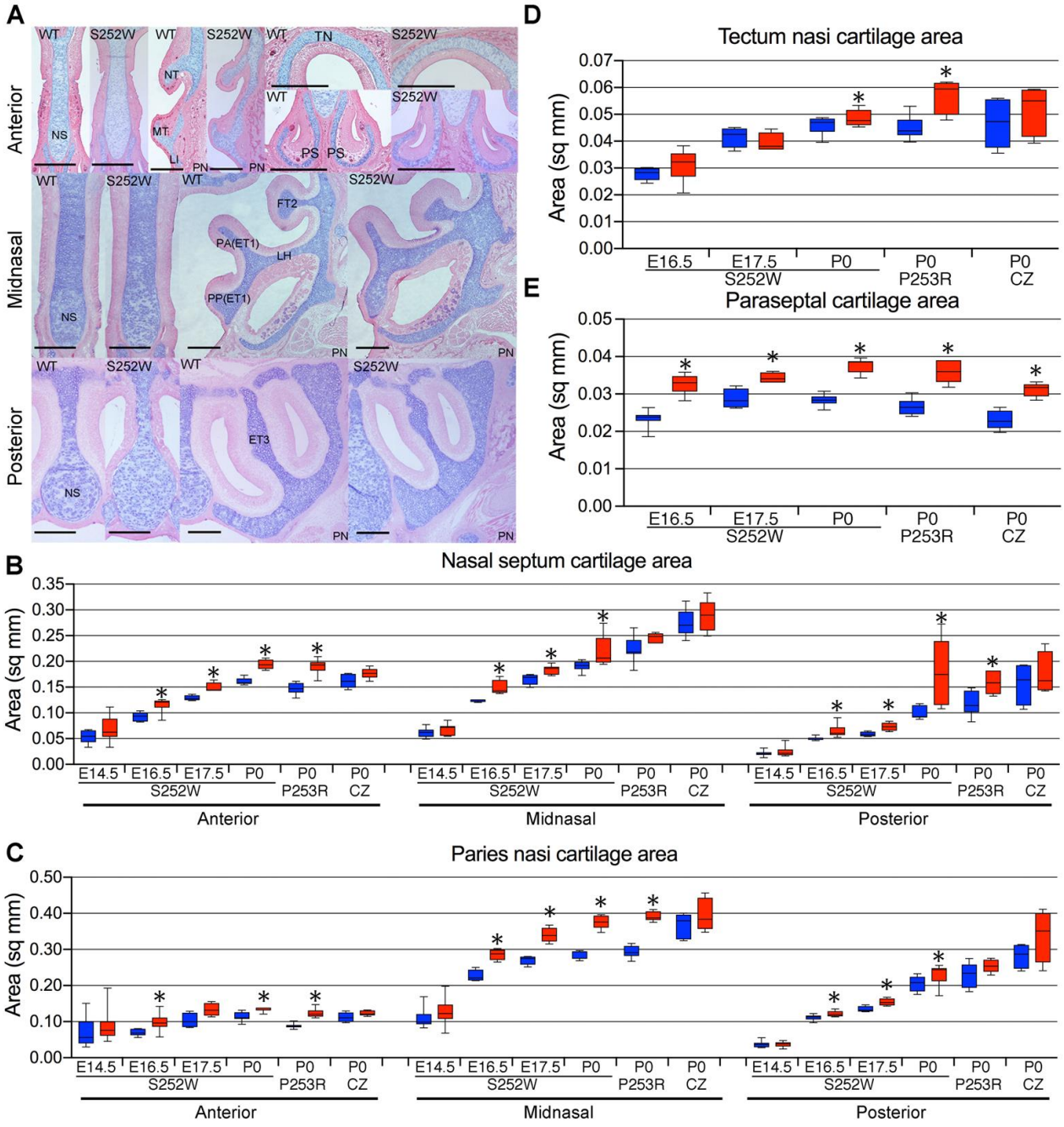

Fig. S3. Nasal septum, paries nasi, tectum nasi, and paraseptal cartilage cross-sectional areas are greater in *Fgfr2* mutant mice. (A) Alcian blue/eosin staining of nasal septum (NS), paries nasi (PN), tectum nasi (TN), and paraseptal cartilages (PS) in the anterior, midnasal, and posterior regions of P0 *Fgfr2*$^{+/+}$ (WT) and Apert *Fgfr2*$^{+/S252W}$ (S252W) mice (TN and PS in anterior only). Scale bars: 250 μm. (B) Nasal septum, (C) Paries nasi, (D) Tectum nasi, and (E) Paraseptal cartilage area measurements. Abbreviations: WT, *Fgfr2*$^{+/+}$; S252W, Apert *Fgfr2*$^{+/S252W}$; P253R, Apert *Fgfr2*$^{+/P253R}$; CZ,

Crouzon *Fgfr2c*$^{C342Y/+}$; ET3, ethmoturbinate 3; FT2, frontoturbinate 2; LH, lamina horizontalis; LI, lamina infraconchalis; MT, maxilloturbinate; NT, nasoturbinate; PA(ET1), pars anterior (ethmoturbinate 1); PP(ET1), pars posterior (ethmoturbinate 1). Blue boxes, WT; red boxes, mutant. *n*=4-18. Data are presented as the median, 25th and 75th percentiles; whiskers indicate minimum and maximum values. **P*<0.05 (Student's *t*-test).

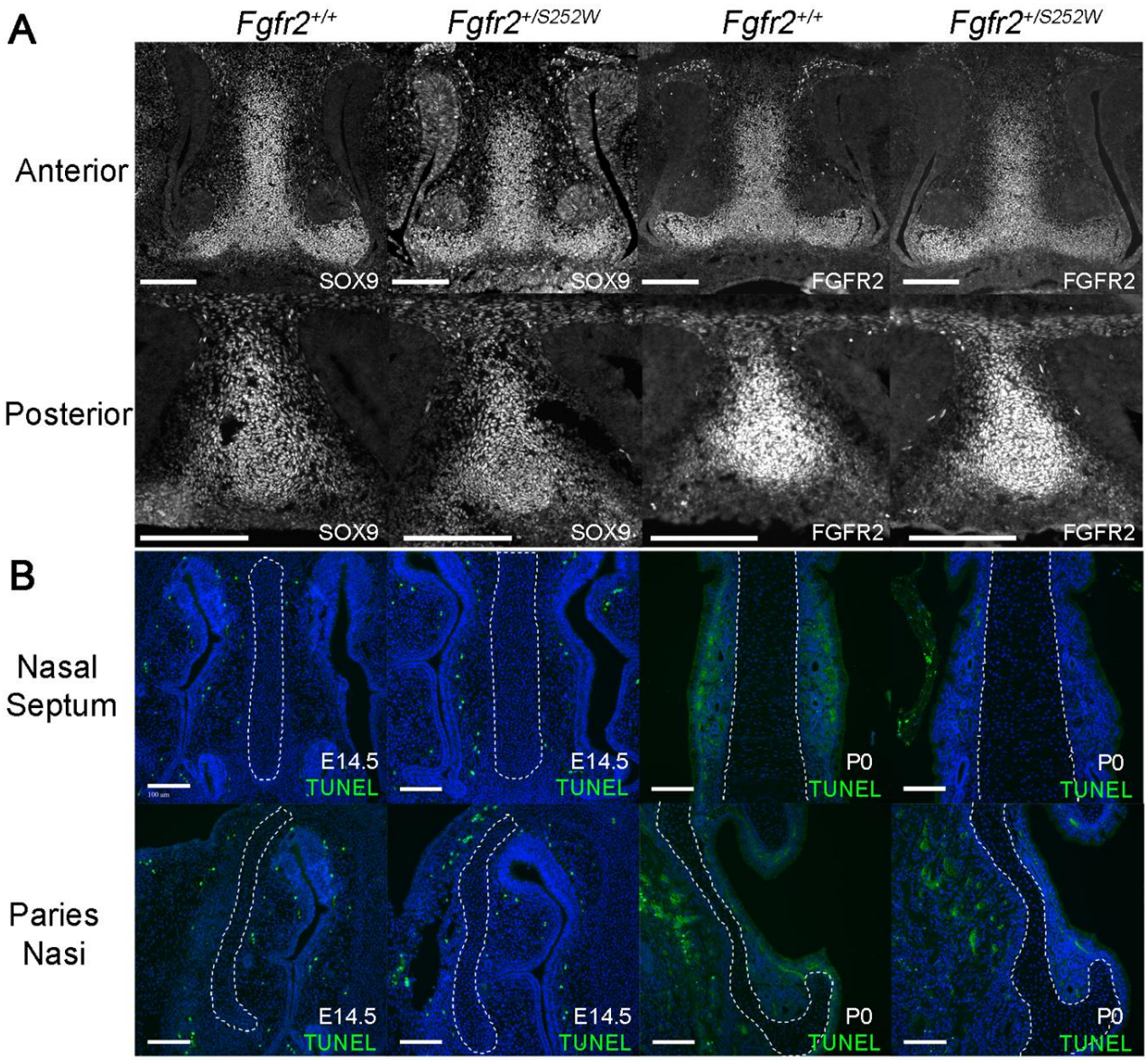

Fig. S4. Neither early nasal septum anlagen size nor apoptosis are affected in Apert *Fgfr2*$^{+/S252W}$ mutants. (A) *Fgfr2*$^{+/+}$ and Apert *Fgfr2*$^{+/S252W}$ anterior and posterior nasal septa immunostained for SOX9 or FGFR2 at E12.5. White signal indicates positive staining in grayscale images. Scale bars: 200 µm. (B) *Fgfr2*$^{+/+}$ and Apert *Fgfr2*$^{+/S252W}$ anterior nasal septa and paries nasi (dashed lines) were assayed for apoptosis using the TUNEL assay (green) at E14.5 and P0. Sections are counterstained with Hoechst 33258. Scale bars: 100 µm.

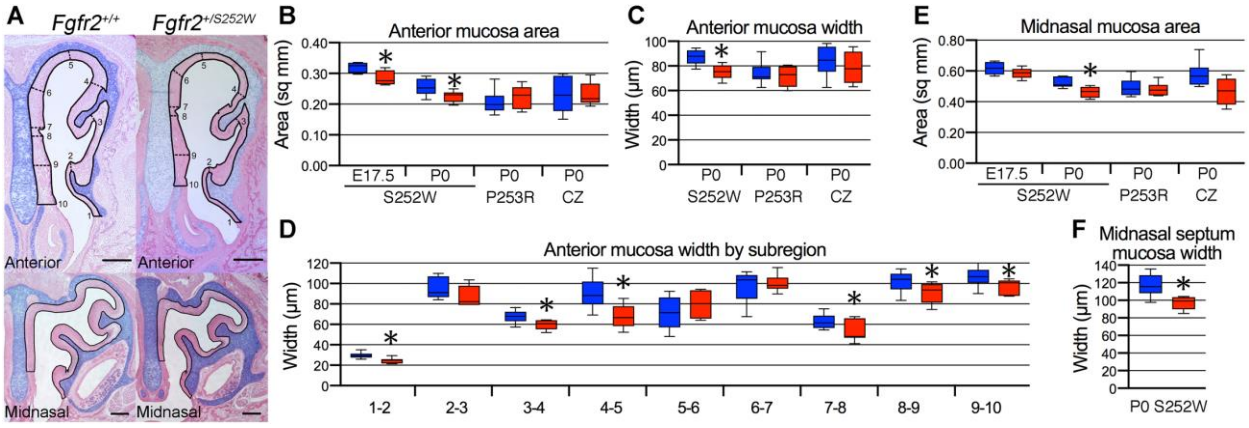

Fig. S5. Nasal mucosa is narrower in Apert *Fgfr2*$^{+/S252W}$ anterior and midnasal regions. (A) Alcian blue/eosin staining of P0 *Fgfr2*$^{+/+}$ and Apert *Fgfr2*$^{+/S252W}$ anterior and midnasal regions with the nasal mucosa area outlined in black and locations of anterior width measurements numbered 1-10. Scale bars: 500 μm. (B) Anterior mucosa area. (C) Anterior mucosa width. (D) Anterior mucosa width by subregion. (E) Midnasal mucosa area. (F) Midnasal mucosa width along the nasal septum. Blue boxes, WT; red boxes, mutant. *n*=4-11. Data are presented as the median, 25th and 75th percentiles; whiskers indicate minimum and maximum values. **P*<0.05 (Student's *t*-test).

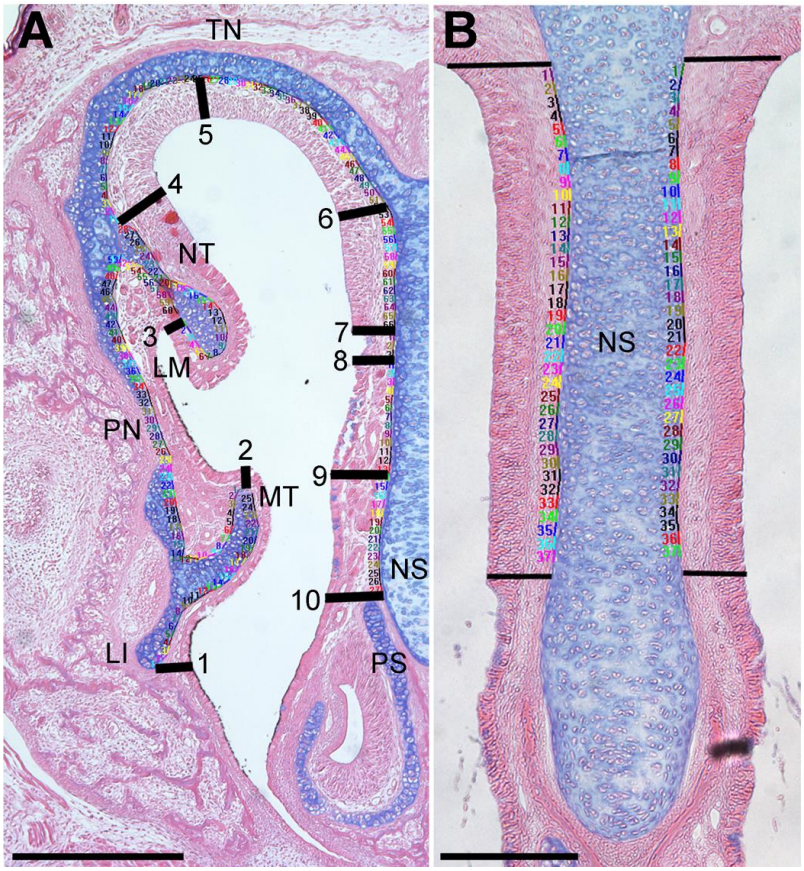

Fig. S6. Landmarks for width measurement of nasal mucosa. (A) Anterior landmarks 1-10 used for measuring mucosal width were placed as follows: 1- a horizontal line from the ventral tip of the lamina infraconchalis (LI) to the nasal space. 2- a vertical line from the most dorsal tip of the maxilloturbinate (MT) to the nasal cavity space. 3- a line from the most dorsal portion of the lateral meatus (LM) to the nasoturbinate (NT), perpendicular to the outer edge of the epithelium. 4- a line from the junction of the NT and paries nasi (PN) to the nasal cavity space, perpendicular to the outer edge of the epithelium. 5- a line from the most dorsal point of tectum nasi (TN) to the nasal cavity space, perpendicular to the outer edge of the epithelium. 6- a line from the junction of the TN and nasal septum (NS) to the nasal cavity space, perpendicular to the outer edge of the epithelium. 7- a horizontal line from the NS to the nasal cavity space, dorsal to the indent in the mucosa. 8- a horizontal line from the NS to the nasal cavity space, ventral to the indent in the mucosa. 9- a horizontal line from the NS to the nasal cavity space at the widest part of the mucosa along the NS. 10- a horizontal line from the NS to the nasal cavity space,

dorsal to the paraseptal cartilage (PS). Segmented regions of 20 μm are indicated by colored numbers. Scale bar: 400 μm. (B) Dorsal and ventral boundaries for measuring mucosal width along the midnasal septum (NS) are indicated by horizontal lines. Segmented regions of 20 μm are indicated by colored numbers. Scale bar: 200 μm.

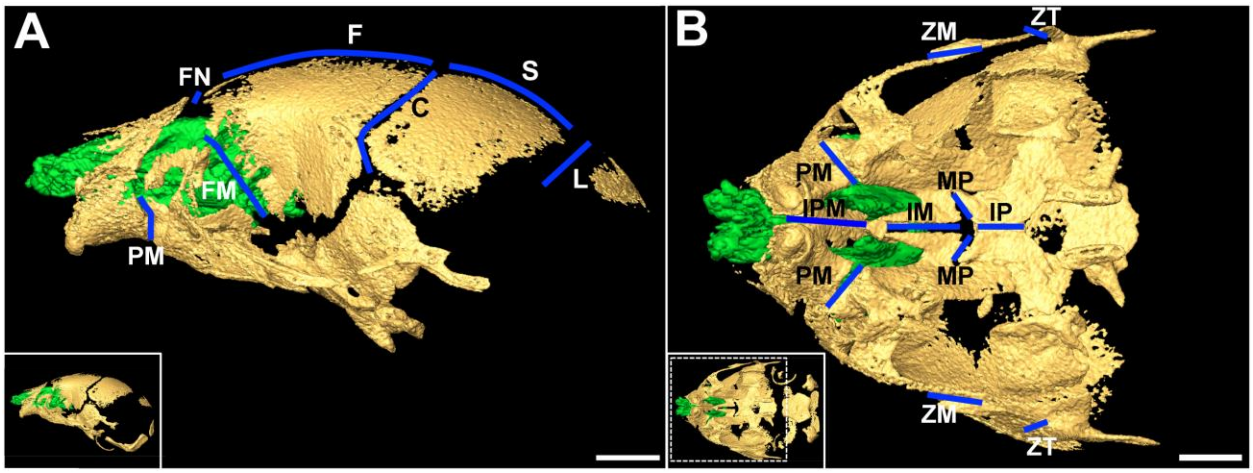

Fig. S7. Relationship between the nasal capsule and craniofacial sutures in the P0 WT mouse. A µCT reconstruction of a partial P0 mouse skull (yellow) is shown superimposed on an MRM reconstruction of the nasal capsule (green) in (A) lateral and (B) ventral view. Dashed box in lower left inset of B shows area of enlargement. Sutures are indicated by blue lines. C, coronal; F, frontal; FM, frontomaxillary; FN, frontonasal; IM, intermaxillary; IP, interpalatine; IPM, interpremaxillary; L, lambdoid; MP, maxillary-palatine; PM, premaxillary-maxillary; S, sagittal; ZM, zygomatic-maxillary; ZT, zygomatic-temporal. Scale bars: 1 mm.

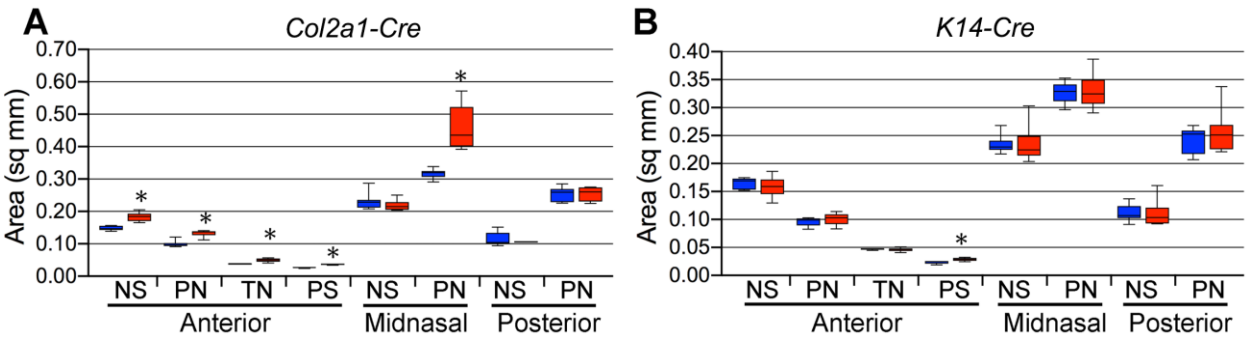

Fig. S8. Areas of cartilage elements in tissue-specific *Cre+;Fgfr2*$^{+/S252W}$ lines at P0 are increased with *Col2a1-Cre*, but not *K14-Cre*. (A) Cartilage element area measurements in WT and *Col2a1-Cre+;Fgfr2*$^{+/S252W}$ mice. (B) Cartilage element area measurements in WT and *K14-Cre+;Fgfr2*$^{+/S252W}$ mice. Abbreviations: NS, nasal septum; PN, paries nasi; TN, tectum nasi; PS, paraseptal cartilage. Blue boxes, WT; red boxes, mutant. *n*=4-11. Data are presented as the median, 25th and 75th percentiles; whiskers indicate minimum and maximum values. **P*<0.05 (Student's *t*-test).

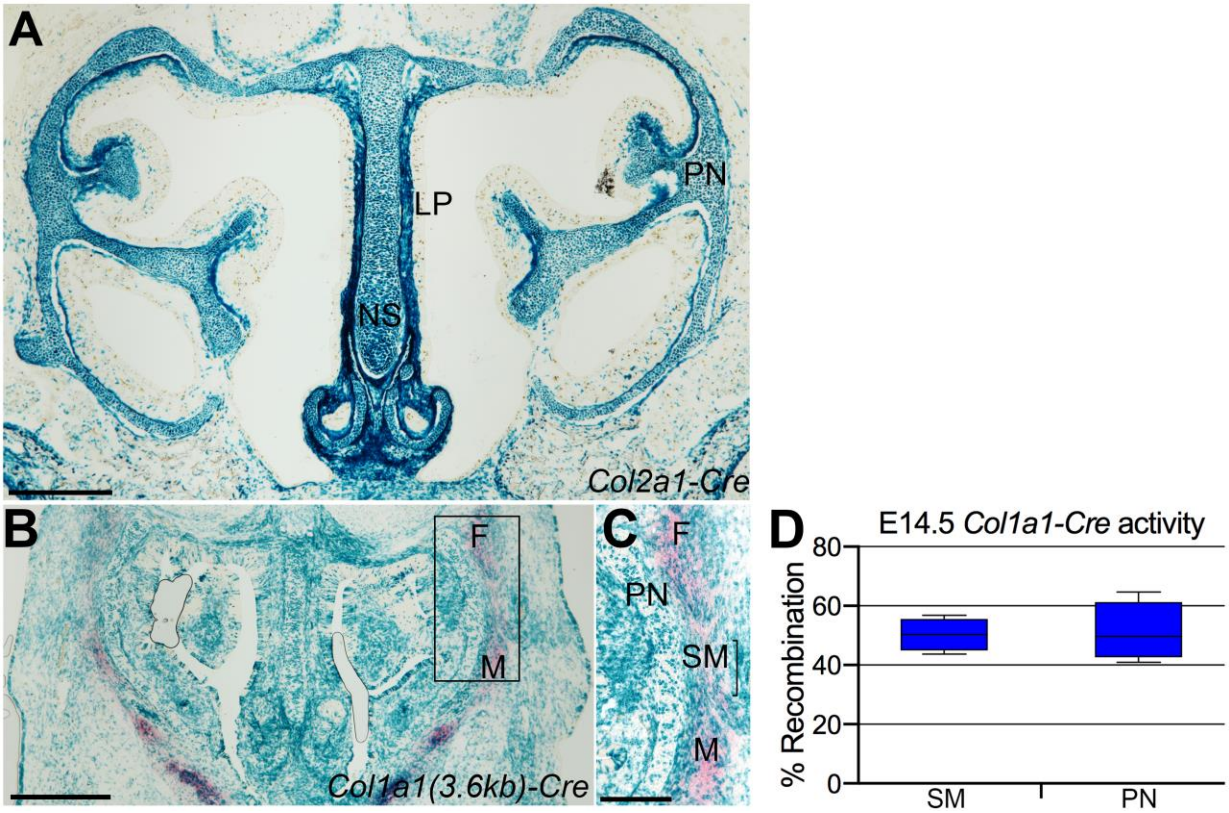

Fig. S9. Expression of *Col2a1- and Col1a1(3.6kb)-Cre*. (A) Coronal section through the midnasal region of a P0 *Col2a1-Cre+;R26R+* head stained for X-gal (blue). *Cre* activity was present throughout nasal capsule cartilage. Strong expression was also present in the lamina propria (LP) adjacent to the nasal septum (NS), and scattered cells throughout the facial mesenchyme. PN, paries nasi. Scale bar: 500 µm. (B) Coronal section through the midnasal region of an E14.5 *Col1a1(3.6kb)-Cre+;R26R+* head stained for X-gal (blue) and ALP (red). Boxed region indicates area shown in C. F, frontal bone anlagen; M, maxillary bone anlagen. Scale bar: 500 µm. (C) Enlargement of boxed area in B. Scale bar: 100 µm. SM, suture mesenchyme. (D) % recombination in *Col1a1(3.6kb)-Cre+;R26R+* frontomaxillary suture mesenchyme and paries nasi cartilage at E14.5. *n*=4. Data are presented as the median, 25th and 75th percentiles; whiskers indicate minimum and maximum values.

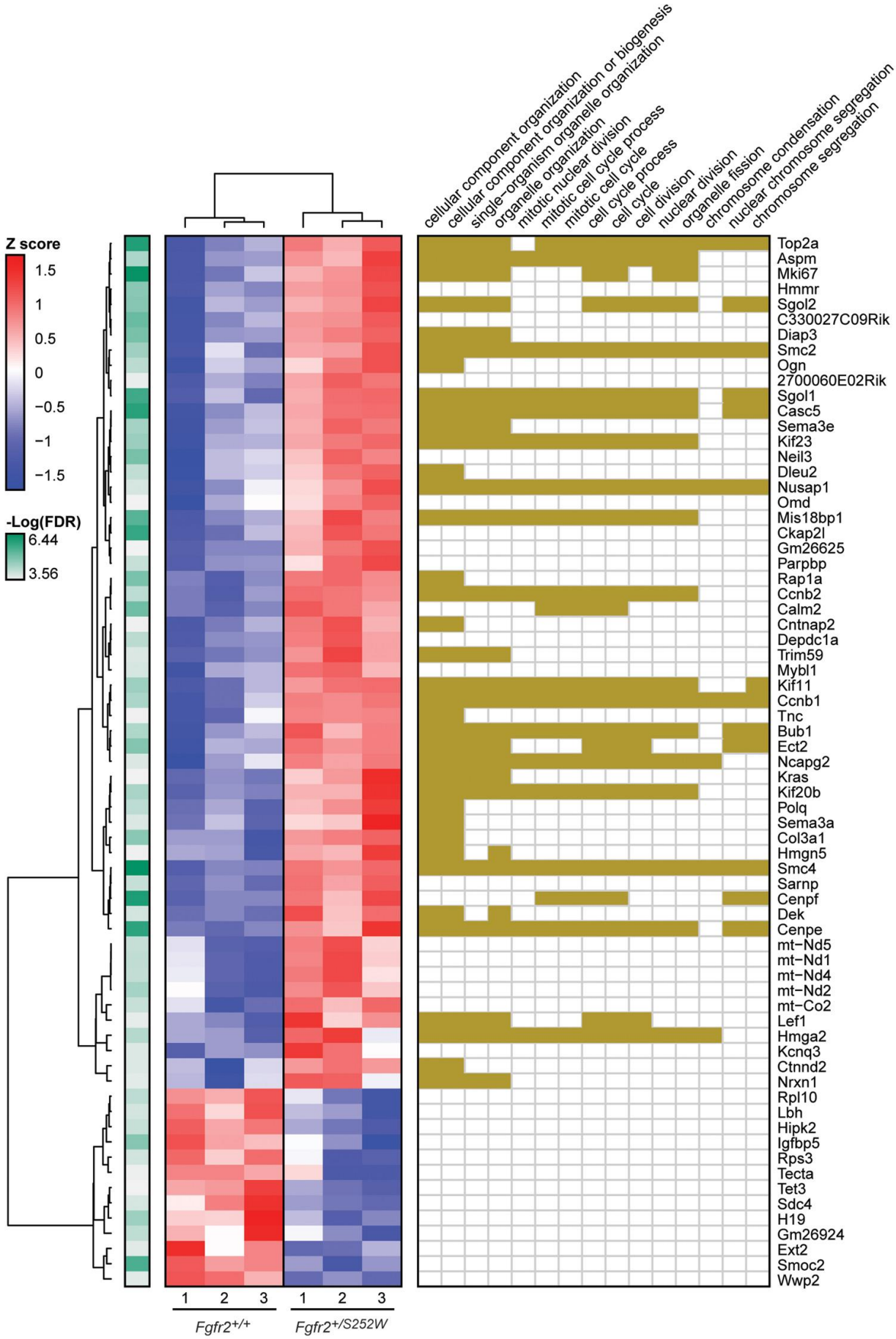
Z score
1.5
1
0.5
0
−0.5
−1
−1.5
-Log(FDR)
6.44
3.56
cellular component organization
cellular component organization or biogenesis
single−organism organelle organization
organelle organization
mitotic nuclear division
mitotic cell cycle process
mitotic cell cycle
cell cycle process
cell cycle
cell division
nuclear division
organelle fission
chromosome condensation
nuclear chromosome segregation
chromosome segregation
Top2a
Aspm
Mki67
Hmmr
Sgol2
C330027C09Rik
Diap3
Smc2
Ogn
2700060E02Rik
Sgol1
Casc5
Sema3e
Kif23
Neil3
Dleu2
Nusap1
Omd
Mis18bp1
Ckap2l
Gm26625
Parpbp
Rap1a
Ccnb2
Calm2
Cntnap2
Depdc1a
Trim59
Mybl1
Kif11
Ccnb1
Tnc
Bub1
Ect2
Ncapg2
Kras
Kif20b
Polq
Sema3a
Col3a1
Hmgn5
Smc4
Sarnp
Cenpf
Dek
Cenpe
mt−Nd5
mt−Nd1
mt−Nd4
mt−Nd2
mt−Co2
Lef1
Hmga2
Kcnq3
Ctnnd2
Nrxn1
Rpl10
Lbh
Hipk2
Igfbp5
Rps3
Tecta
Tet3
Sdc4
H19
Gm26924
Ext2
Smoc2
Wwp2
1 2 3 1 2 3
Fgfr2+/+
Fgfr2+/S252W

Fig. S10. Differential gene expression at E14.5 in Apert *Fgfr2*$^{+/S252W}$ nasal cartilage. (Left) Heat map shows hierarchical clustering of genes differentially expressed genes in Apert *Fgfr2*$^{+/S252W}$ nasal cartilage compared to WT (FDR <0.05). Rows show the change in expression converted to a Z-score (red/blue, color key on left) and columns represent different, replicate experimental samples (labeled at bottom). FDR adjusted *P*-values are shown in green (color key on left). (Right) Gene Ontology Biological Process (GO BP) terms associated with each gene are shown (brown) for significantly (*P*<0.05) enriched GO BP terms.

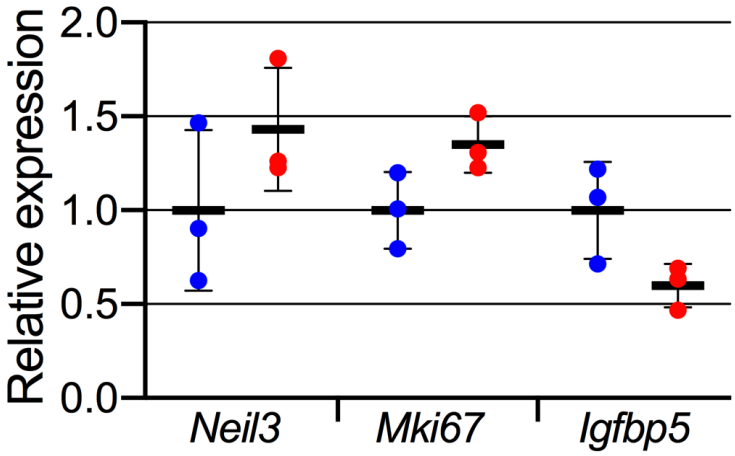

Fig. S11. RT-qPCR validation of differential gene expression at E14.5 in Apert *Fgfr2*$^{+/S252W}$ nasal cartilage. Relative expression of the indicated genes in the E14.5 anterior nasal septum was compared between WT (blue; *n*=3) and Apert *Fgfr2*$^{+/S252W}$ mutants (red; *n*=3) embryos. Black bars indicate mean and standard deviation. *P*-values (Student's *t*-test) are 0.24 (*Neil3*), 0.07 (*Mki67*), and 0.07 (*Igfbp5*).

Table S1. Summary of features of craniosynostosis mouse models used in study.

Feature	Apert *Fgfr2*$^{+/S252W}$	Apert *Fgfr2*$^{+/P253R}$	Crouzon/Pfeiffer *Fgfr2c*$^{C342Y/+}$
***Cre*-dependent expression**	yes	yes	no
Isoforms affected	epithelial, mesenchymal	epithelial, mesenchymal	mesenchymal
Background	C57BL/6J	C57BL/6J	CD1
Perinatal lethality	yes	yes	no
Facial sutures fusing at E17.5[A]	frontomaxillary; premaxillary-maxillary	frontomaxillary; premaxillary-maxillary	not determined
Facial sutures fusing at P0[B]	all except the intermaxillary	all except intermaxillary	interpremaxillary; maxillary-palatine
Calvarial sutures fusing at E17.5	coronal	coronal	coronal
Calvarial sutures fusing at P0	coronal	coronal	coronal

[A] Suture information is summarized from Martinez-Abadias et al., 2010, 2013b and Motch Perrine et al., 2014. For each genotype, suture patency is variable across mice examined within developmental ages. Sutures listed here as "fusing" were fusing or completely fused in at least 20% of mice examined in a genotype group. See publications for more detailed analysis of variation in timing and extent of fusion for individual sutures and genotypes.

[B] "all" includes the following sutures: premaxillary-maxillary, zygomatic-maxillary, maxillary-palatine, frontomaxillary. Facial sutures that were scored but that did not show fusion in at least 10% of the Apert syndrome mouse models examined include: intermaxillary, interpremaxillary, interpalatine, frontopremaxillary, and frontonasal. The interpremaxillary suture fuses in WT and Crouzon *Fgfr2c*$^{C342Y/+}$ mice. Difference in suture closure patterns in the two Apert syndrome models is one of degree rather than kind with similar numbers of mice showing fusion in most sutures, excepting the maxillary-palatine suture and the frontomaxillary suture where a greater number of mice show fusion in the Apert *Fgfr2*$^{+/S252W}$ model. The facial sutures of Crouzon *Fgfr2c*$^{C342Y/+}$ mice tend to fuse later than the facial sutures in either Apert syndrome model, and the Crouzon *Fgfr2c*$^{C342Y/+}$ facial phenotype is not as apparent at birth relative to the two Apert models.

Table S2. Statistical comparison of linear dimensions of the nasal passages in the Apert *Fgfr2*$^{+/S252W}$ model.

Age	Dimension	*n* WT*	*n* MT‡	WT distance (mean±s.e.m.)§	MT distance (mean±s.e.m.)§	WT vs MT (*P*-value)	WT P0 vs E17.5 (*P*-value)	MT P0 vs E17.5 (*P*-value)
E17.5	**Length**	6	5	3.97 ± 0.07	3.86 ± 0.11	0.329	-	-
	Width	6	5	2.51 ± 0.02	2.33 ± 0.10	0.177	-	-
	Height	6	5	1.61 ± 0.05	1.57 ± 0.01	0.429	-	-
P0	**Length**	5	5	4.21 ± 0.16	4.16 ± 0.12	0.841	0.429	0.095
	Width	5	5	2.97 ± 0.10	2.50 ± 0.04	0.008	0.004	0.222
	Height	5	5	1.91 ± 0.08	1.51 ± 0.11	0.032	0.030	0.151

*WT, unaffected. ‡MT, mutant. §Distances in mm; s.e.m., standard error of the mean.

Table S3. Statistical comparison of the nasal passage airspace volume of the *Col2a1-Cre+;Fgfr2*$^{+/S252W}$ line.

Age	*n* WT; *Col2a1-Cre+;Fgfr2*$^{+/+}$	*n* MT; *Col2a1-Cre+;Fgfr2*$^{+/S252W}$	WT volume (mean±s.e.m.)*	MT volume (mean±s.e.m.)*	WT vs MT (*P*-value)
P0	5	5	2.72 ± 0.10	2.60 ± 0.09	0.42

*Volumes are in mm^3; s.e.m., standard error of the mean.

Table S4. Differential gene expression in Apert *Fgfr2*$^{+/S252W}$ E14.5 nasal septum cartilage, relative to unaffected littermates (FDR<0.05).

Gene Symbol[A]	Ensembl ID	Average WT Log2 FPKM	Log2 fold change	False Discovery Rate
Omd	ENSMUSG00000048368	3.89	2.11	0.047
Sema3e	ENSMUSG00000063531	4.39	1.61	0.016
Neil3	ENSMUSG00000039396	6.67	1.48	0.009
Ect2	ENSMUSG00000027699	4.94	1.47	0.010
Lef1	ENSMUSG00000027985	4.19	1.43	0.042
Nrxn1	ENSMUSG00000024109	5.52	1.37	0.039
Diap3	ENSMUSG00000022021	5.21	1.35	0.009
Sgol1	ENSMUSG00000023940	5.99	1.32	0.003
Depdc1a	ENSMUSG00000028175	4.60	1.30	0.022
Ckap2l	ENSMUSG00000048327	6.49	1.28	0.003
Casc5	ENSMUSG00000027326	7.13	1.22	0.003
Polq	ENSMUSG00000034206	5.05	1.22	0.022
Sgol2	ENSMUSG00000026039	6.01	1.21	0.010
C330027C09Rik	ENSMUSG00000033031	6.06	1.19	0.007
Kcnq3	ENSMUSG00000056258	5.13	1.18	0.034
Mis18bp1	ENSMUSG00000047534	6.85	1.14	0.005
Sema3a	ENSMUSG00000028883	5.92	1.13	0.033
Dleu2	ENSMUSG00000097589	6.18	1.11	0.023
Trim59	ENSMUSG00000034317	4.89	1.11	0.033
mt-Co2	ENSMUSG00000064354	5.55	1.10	0.024
Parpbp	ENSMUSG00000035365	5.59	1.09	0.023
Cntnap2	ENSMUSG00000039419	4.83	1.09	0.047
Cenpe	ENSMUSG00000045328	7.82	1.07	0.003
Hmgn5	ENSMUSG00000031245	5.17	1.06	0.047
Cenpf	ENSMUSG00000026605	7.65	1.05	0.003
Mki67	ENSMUSG00000031004	10.36	1.05	0.002
Kif23	ENSMUSG00000032254	6.27	1.05	0.015
Bub1	ENSMUSG00000027379	5.98	1.05	0.018
Ccnb1	ENSMUSG00000041431	5.84	1.04	0.017
Sarnp	ENSMUSG00000078427	5.28	1.03	0.023
Hmmr	ENSMUSG00000020330	6.25	1.02	0.010
Nusap1	ENSMUSG00000027306	6.66	1.01	0.031
Ccnb2	ENSMUSG00000032218	5.60	0.99	0.022
Top2a	ENSMUSG00000020914	8.64	0.98	0.003
Ctnnd2	ENSMUSG00000022240	6.23	0.98	0.034
Ncapg2	ENSMUSG00000042029	6.12	0.98	0.033
Smc4	ENSMUSG00000034349	8.26	0.96	0.002
Kif20b	ENSMUSG00000024795	6.51	0.95	0.017
Ogn	ENSMUSG00000021390	7.34	0.92	0.022

Smc2	ENSMUSG00000028312	7.53	0.88	0.015
Mybl1	ENSMUSG00000025912	6.42	0.86	0.031
Aspm	ENSMUSG00000033952	7.24	0.83	0.017
Kif11	ENSMUSG00000012443	7.25	0.81	0.015
Rap1a	ENSMUSG00000068798	7.81	0.78	0.009
Hmga2	ENSMUSG00000056758	9.80	0.76	0.019
Gm26625	ENSMUSG00000097138	6.48	0.73	0.049
mt-Nd2	ENSMUSG00000064345	11.58	0.72	0.016
Calm2	ENSMUSG00000036438	8.92	0.72	0.008
Col3a1	ENSMUSG00000026043	8.96	0.71	0.010
2700060E02Rik	ENSMUSG00000021807	7.26	0.67	0.043
Tnc	ENSMUSG00000028364	8.00	0.65	0.047
Kras	ENSMUSG00000030265	7.82	0.63	0.047
mt-Nd4	ENSMUSG00000064363	12.54	0.59	0.023
Dek	ENSMUSG00000021377	9.08	0.57	0.031
mt-Nd1	ENSMUSG00000064341	12.92	0.55	0.023
mt-Nd5	ENSMUSG00000064367	13.23	0.52	0.023
Wwp2	ENSMUSG00000031930	10.04	-0.50	0.038
Tet3	ENSMUSG00000034832	7.30	-0.67	0.047
Hipk2	ENSMUSG00000061436	7.86	-0.68	0.023
Rpl10	ENSMUSG00000008682	8.13	-0.77	0.022
H19	ENSMUSG00000000031	11.74	-0.77	0.015
Ext2	ENSMUSG00000027198	7.35	-0.80	0.038
Rps3	ENSMUSG00000030744	7.54	-0.82	0.031
Sdc4	ENSMUSG00000017009	6.49	-0.95	0.031
Igfbp5	ENSMUSG00000026185	11.37	-1.02	0.010
Lbh	ENSMUSG00000024063	5.89	-1.04	0.031
Smoc2	ENSMUSG00000023886	6.64	-1.14	0.004
Gm26924	ENSMUSG00000098178	14.61	-1.18	0.023
Tecta	ENSMUSG00000037705	0.89	-3.58	0.047

[A] Genes in **bold** (24/69) were identified as enriched in Biological Process categories related to regulation of the chromosome or cell cycle. Genes underlined (26/69) were linked to regulation of the cell cycle by literature search.

Table S5. Differential expression of select *Fgf*, *Fgfr*, and *Sox* genes in Apert *Fgfr2*$^{+/S252W}$ E14.5 nasal septum cartilage, relative to unaffected littermates.

Gene Symbol	Ensembl ID	Average WT Log2 FPKM	Log2 fold change	False Discovery Rate
Fgf2	ENSMUSG00000037225	4.97	-0.09	0.913
Fgf11	ENSMUSG00000042826	2.41	0.06	0.967
Fgf12	ENSMUSG00000022523	0.92	-2.27	0.278
Fgf13	ENSMUSG00000031137	0.662	-0.03	0.992
Fgfr1	ENSMUSG00000031565	6.03	-0.18	0.643
Fgfr2	ENSMUSG00000030849	7.68	-0.27	0.395
Fgfr3	ENSMUSG00000054252	5.15	-0.01	0.989
Fgfr4	ENSMUSG00000005320	2.40	-0.72	0.470
Sox5	ENSMUSG00000041540	8.09	-0.11	0.752
Sox6	ENSMUSG00000051910	7.22	-0.10	0.786
Sox9	ENSMUSG00000000567	8.06	-0.69	0.057

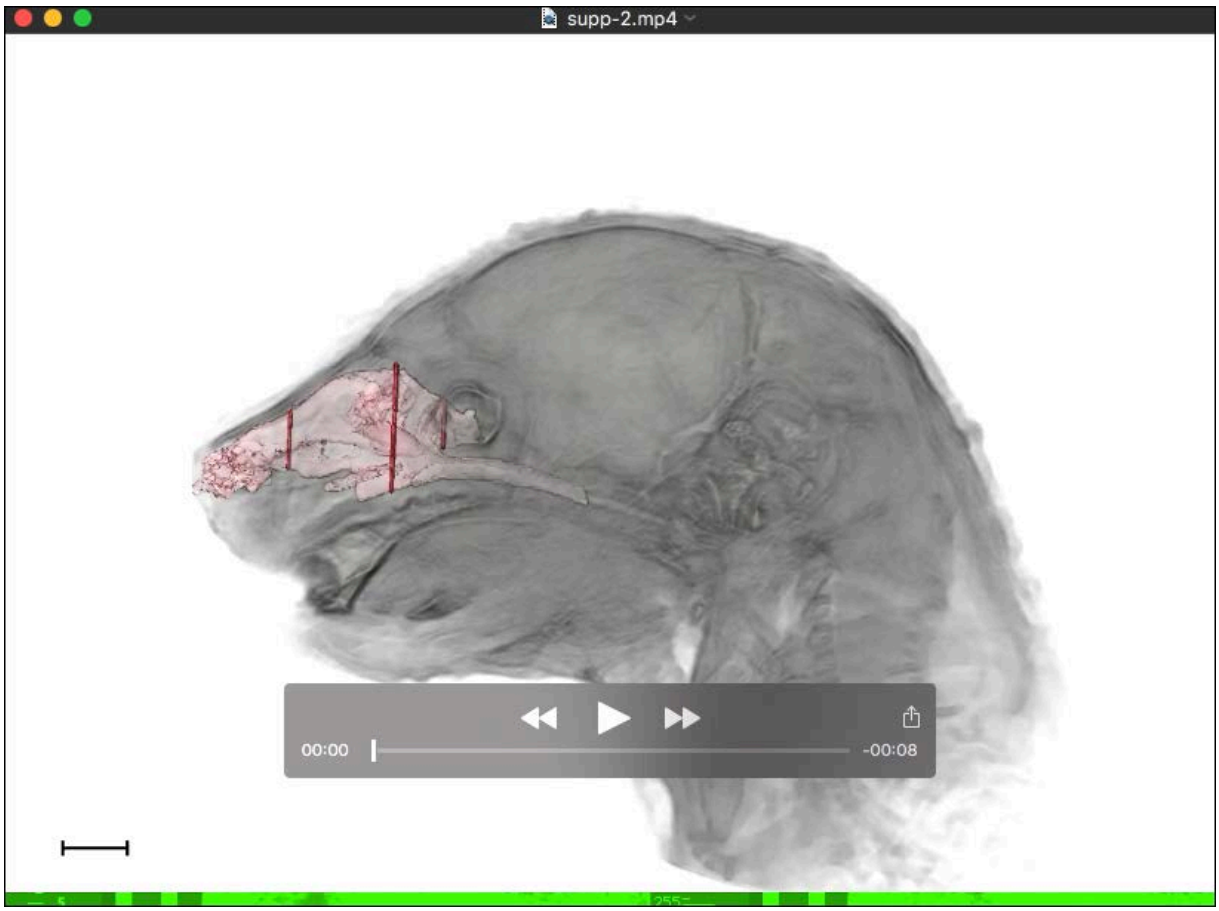

Movie 1. 3D MRM rendering of an unaffected, P0 *Fgfr2*$^{+/+}$ mouse head. The nasal passages and nasopharyngeal duct are shown in pink. The anterior, midnasal and posterior nasal slices corresponding to the locations described in Fig. 1 are indicated in red.

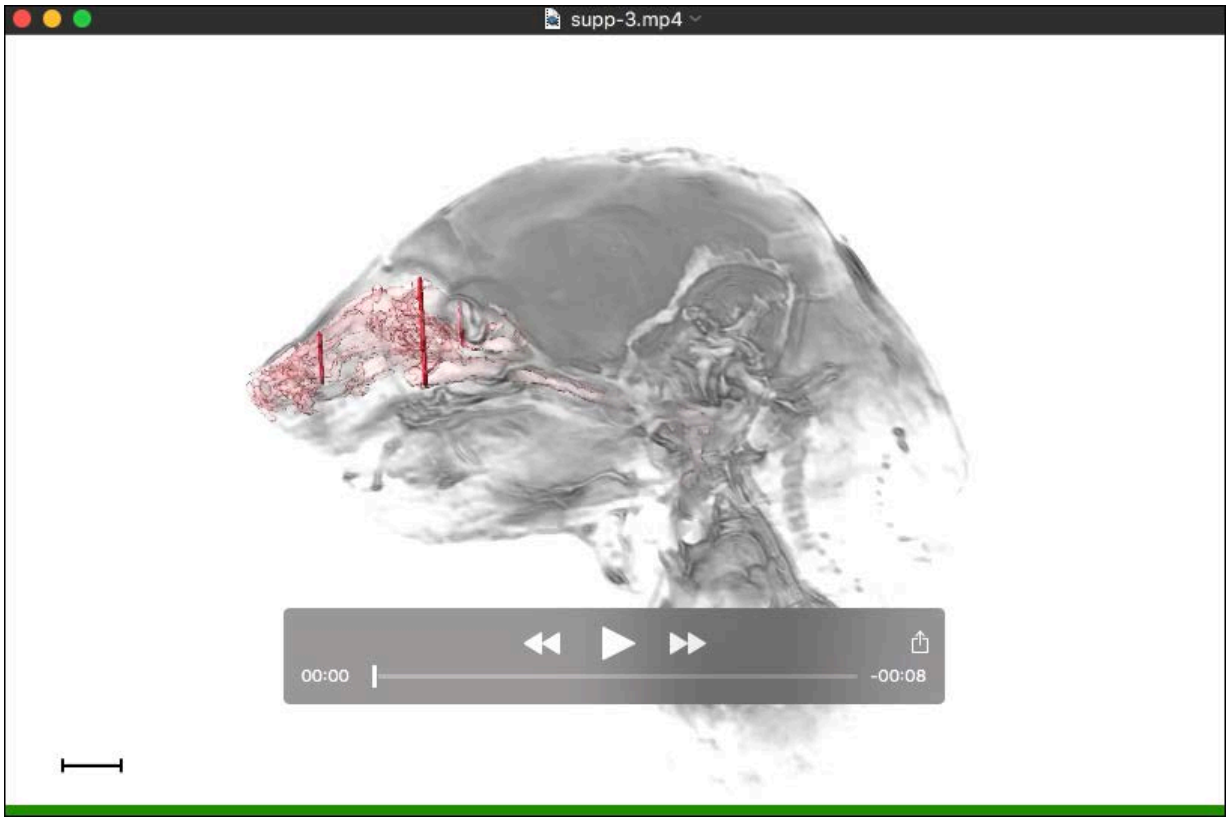

Movie 2. 3D MRM rendering of a P0 Apert *Fgfr2*$^{+/S252W}$ mouse head. The nasal passages and nasopharyngeal duct are shown in pink. The anterior, midnasal and posterior nasal slices corresponding to the locations described in Fig. 1 are indicated in red.